



15 **Contents**

16 **1. Table.**

17 **Table S1.** Some representative examples of efficient luminescent MOF sensors for 2,4-  
18 DNP.

19 **2. Figures**

20 **Fig. S1.** high-resolution (a-b) SEM and (c) TEM images of NH<sub>2</sub>-MIL-125(Ti).

21 **Fig. S2.** (a) Full range XPS spectrum of NH<sub>2</sub>-MIL-125(Ti) after the reaction with 2,4-  
22 DNP, XPS spectra of NH<sub>2</sub>-MIL-125(Ti) before and after the reaction with 2,4-DNP in  
23 the: (b) C 1s, and (c) O 1s.

24 **Fig. S3.** (a) The excitation spectrum and (b) emission spectrum of NH<sub>2</sub>-MIL-125(Ti)  
25 dispersed in water.

26 **Fig. S4.** The correlation curve between I<sub>0</sub>/I and the concentration of 2,4-DNP was  
27 obtained by the Stern-Volmer equation.

28 **Fig. S5.** (a) Fluorescence emission spectra, and (b) the corresponding plot of  
29 fluorescence intensity versus analyte concentration of 2,4-DNP in MOF suspension  
30 (0.09 mg mL<sup>-1</sup>).

31 **Fig. S6.** PL emission spectra of NH<sub>2</sub>-MIL-125(Ti) in the presence of various  
32 concentrations of aromatic compounds upon excitation at 334 nm.

33 **Fig. S7.** (I<sub>0</sub>-I)/I<sub>0</sub> values (i.e., quenching efficiency) of NH<sub>2</sub>-MIL-125(Ti) suspension in  
34 the presence of different aromatic compounds (310 μM).

35 **Fig. S8.** PL emission spectra of NH<sub>2</sub>-MIL-125(Ti) in the presence of 2,4-DNP and other  
36 aromatic compounds upon excitation at 334 nm.

37 **Fig. S9.** PL emission spectra of NH<sub>2</sub>-MIL-125(Ti) in the presence of 2,4-DNP and  
38 various metal salts upon excitation at 334 nm.

39 **Fig. S10.** The anti-interference test of NH<sub>2</sub>-MIL-125(Ti) in the detection of 2,4-DNP.

40 **Fig. S11.** A real sample test was conducted in tap water.

41 **Fig. S12.** Fluorescence lifetime of NH<sub>2</sub>-MIL-125(Ti) before and after reaction with 70  
42 μM 2,4-DNP.

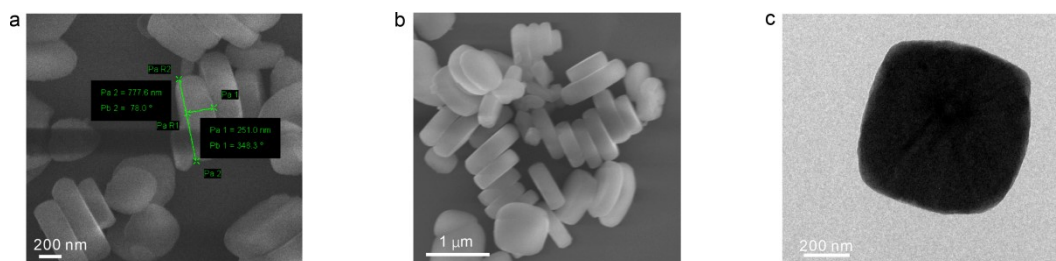
43 **Fig. S13.** (a) The relationship between B/B<sub>0</sub>, (b) L/L<sub>0</sub> values and different  
44 concentrations of 2,4-DNP (blue) and 1,4-DNB (gray) (B and L values were identified  
45 by APP Color Detector under the irradiation of 365nm UV lamp).

46

47 **Table S1.** Some representative examples of efficient luminescent MOF sensors for  
 48 2,4-DNP.

Order	MOF	LOD ( $\mu\text{g L}^{-1}$ )	Ksv	Linear range ( $\mu\text{M}$ )	Parameters for selectivity	Ref.
1	Eu@MOF-253	1.84	$4.2 \times 10^4 \text{ M}^{-1}$	0-100	fluorescence intensity	1
2	FJI-C8 (Zn-MOF)	530	$5.11 \times 10^4 \text{ M}^{-1}$	0-5	fluorescence intensity	2
3	$[\text{Y}_2(\text{PIA})_3(\text{DMF})_3(\text{C}_6\text{H}_5\text{OH})]$	84.69	$3.63 \times 10^4 \text{ M}^{-1}$	/	/	3
4	$\{\text{Zn}_2(\text{NDC})_2(\text{AzoAEpP}) \cdot 2\text{DMF}\}_n$	1120	$8.93 \times 10^3 \text{ M}^{-1}$	/	/	4
5	$[\text{Zn}_2(\text{oba})_4(4,4'\text{-bpy})_2]_n$	370	$6.35 \times 10^3 \text{ M}^{-1}$	0-35	fluorescence intensity	5
6	$\text{Mg}_{24}(\text{TC}_4\text{A})_6(\text{BTC})_8(\text{H}_2\text{O})_6$	379.26	$3.98 \times 10^4 \text{ M}^{-1}$	0-40	/	6
7	$\text{NH}_2\text{-MIL-125(Ti)}$	186.27	$2.002 \times 10^4 \text{ M}^{-1}$	0-70	fluorescence intensity	This work
		602.61	$1.8 \times 10^5 \text{ nm} \cdot \text{M}^{-1}$		emission peak shift	

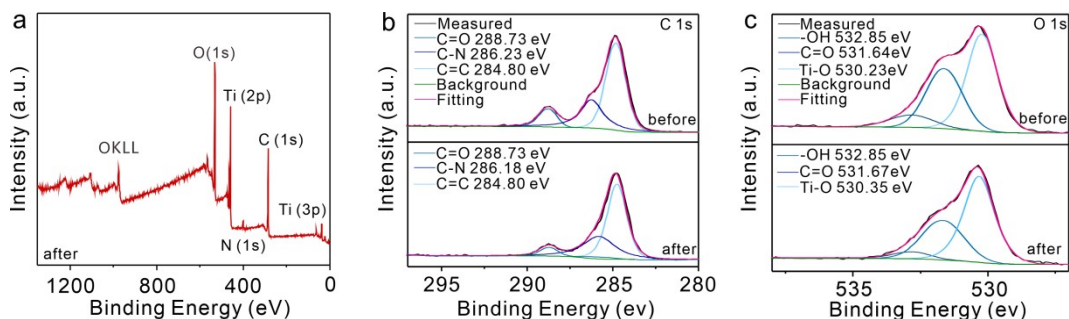
49



50

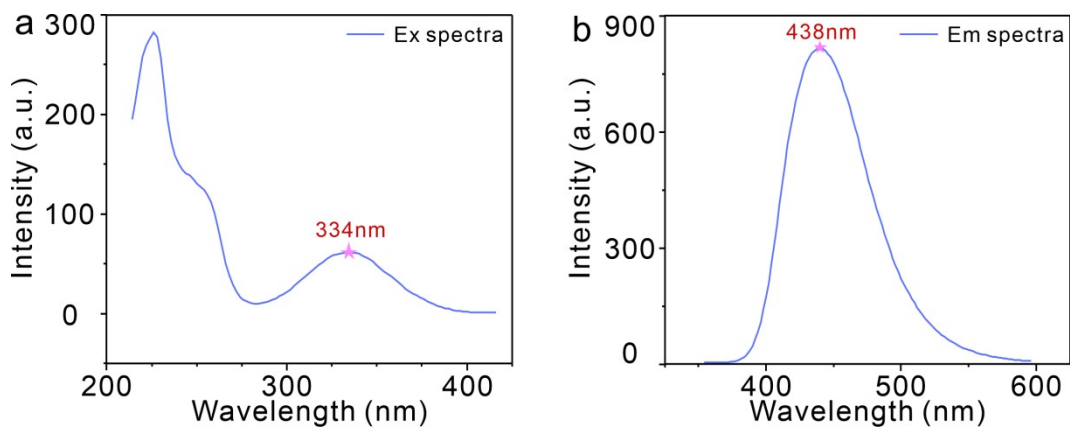
51 **Fig. S1.** high-resolution (a-b) SEM and (c) TEM images of  $\text{NH}_2\text{-MIL-125(Ti)}$ .

52

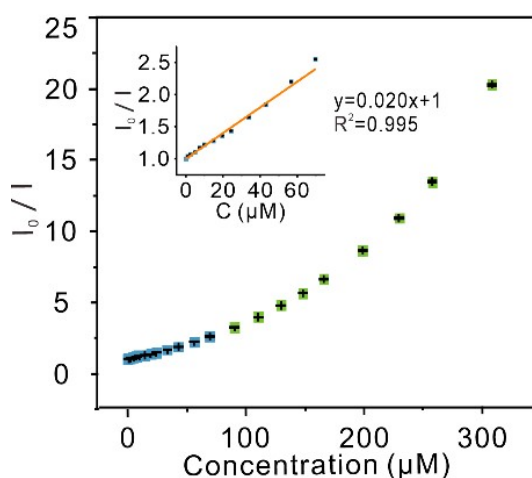


53

54 **Fig. S2.** (a) Full range XPS spectrum of  $\text{NH}_2\text{-MIL-125(Ti)}$  after the reaction with 2,4-  
 55 DNP, XPS spectra of  $\text{NH}_2\text{-MIL-125(Ti)}$  before and after the reaction with 2,4-DNP in  
 56 the: (b) C 1s, and (c) O 1s.

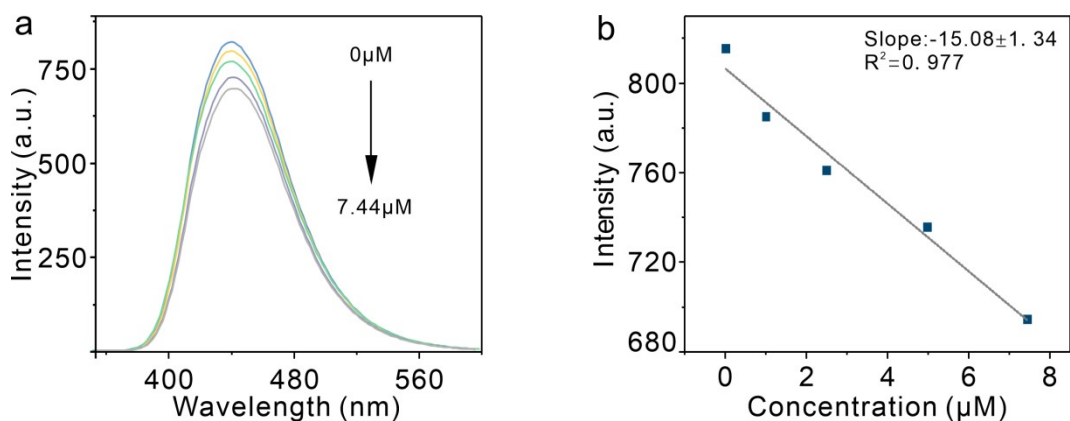


57  
 58 **Fig. S3.** (a)The excitation spectrum and (b)emission spectrum of NH<sub>2</sub>-MIL-125(Ti)  
 59 dispersed in water.  
 60



61  
 62 **Fig. S4.** The correlation curve between I<sub>0</sub>/I and the concentration of 2,4-DNP was  
 63 obtained by the Stern-Volmer equation. A linear relation is shown in the low  
 64 concentration region (see the inset in **Fig. S4**).  
 65

66 The fluorescence quenching efficiency can be quantitatively explained by the  
 67 Stern–Volmer (SV) equation:  $I_0 / I = 1 + K_{sv} [Q]$ , where  $K_{sv}$  is the quenching constant  
 68 ( $M^{-1}$ ),  $[Q]$  is the molar concentration of analyte, and  $I_0$  and  $I$  are the fluorescence  
 69 intensity before and after adding analyte, respectively (**Fig. S4**). The fluorescence  
 70 emission peak shift ( $\Delta\lambda$ ) of the MOF before and after adding the analyte can be  
 71 described by  $\Delta\lambda = K_{sv} [Q]$ , where  $K_{sv}$  represents the quenching constant ( $M^{-1}$ ),  $[Q]$   
 72 denotes the molar concentration of the analyte (**Fig. 2c**).



73

74 **Fig. S5.** (a) Fluorescence emission spectra, and (b) the corresponding plot of  
 75 fluorescence intensity versus analyte concentration of 2,4-DNP in MOF suspension  
 76 ( $0.09 \text{ mg mL}^{-1}$ )

77

78 With the fluorescence intensity as a parameter, the Limit of Detection (LOD) for

79 2,4-DNP in the  $\text{NH}_2\text{-MIL-125(Ti)}$  aqueous phase ( $3\sigma$  rule):

80  $\text{LOD} = 3 \cdot \sigma / S$

81  $= 3 \cdot 1.53 / 15.08$

82  $= 304.38 \text{ nM} (186.27 \text{ } \mu\text{g L}^{-1})$

83 The fluorescence spectra of the  $\text{NH}_2\text{-MIL-125(Ti)}$  suspension were recorded

84 multiple times ( $n=11$ ) with blank samples. The standard deviation  $\sigma$  of fluorescence

85 intensity for the blank probe, without the addition of 2,4-DNP, was calculated to be

86 1.53.

87 With the emission peak wavelength as a parameter, the Limit of Detection (LOD)

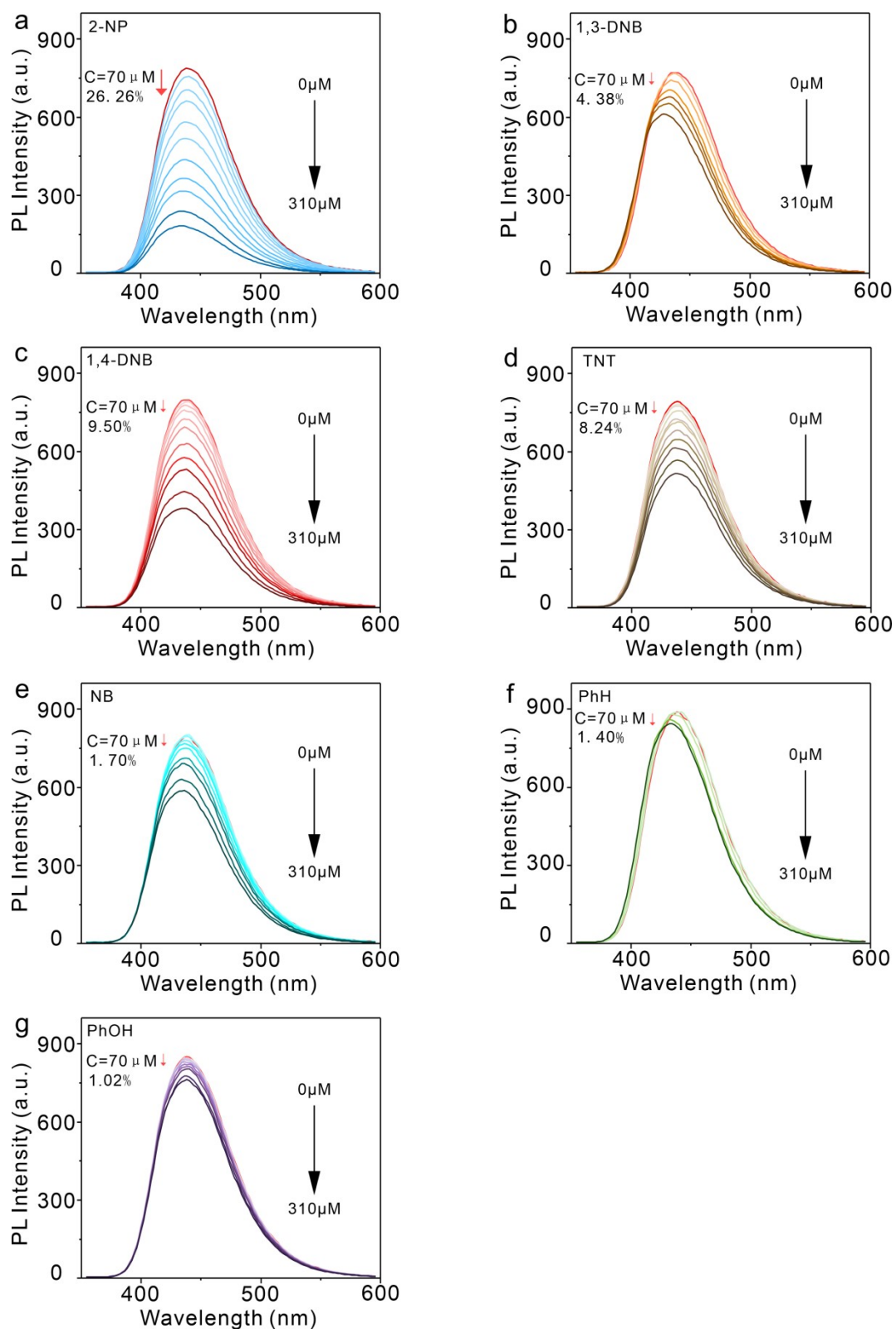
88 for 2,4-DNP in the  $\text{NH}_2\text{-MIL-125(Ti)}$  aqueous phase (signal-to-noise ratio, SNR):

89  $\text{LOD} = 0.99 \text{ } \mu\text{M} (602.61 \text{ } \mu\text{g L}^{-1})$ .

90 The SNR was equal to 3.

91 Two approaches were used to determine LODs due to the discrepancy between

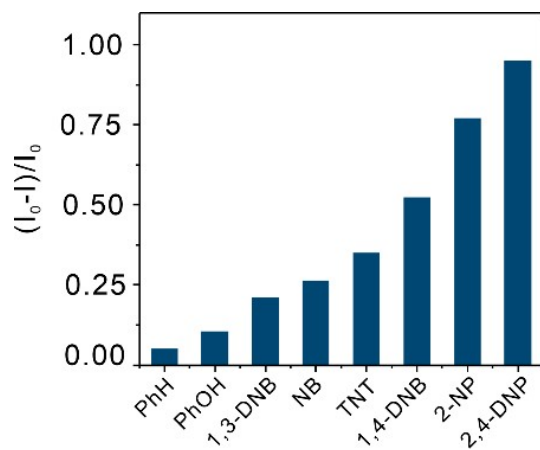
92 fluorescence intensity and Stoker shift signal.



93

94 **Fig. S6.** PL emission spectra of  $\text{NH}_2\text{-MIL-125(Ti)}$  in the presence of various  
 95 concentrations of (a) 2-NP, (b) 1,3-DNB, (c) 1,4-DNB, (d) TNT, (e) NB, (f) PhH and  
 96 (g) PhOH upon excitation at 334 nm (the figures showed the quenching efficiency when  
 97 analyte concentration was 70  $\mu\text{M}$ ).

98



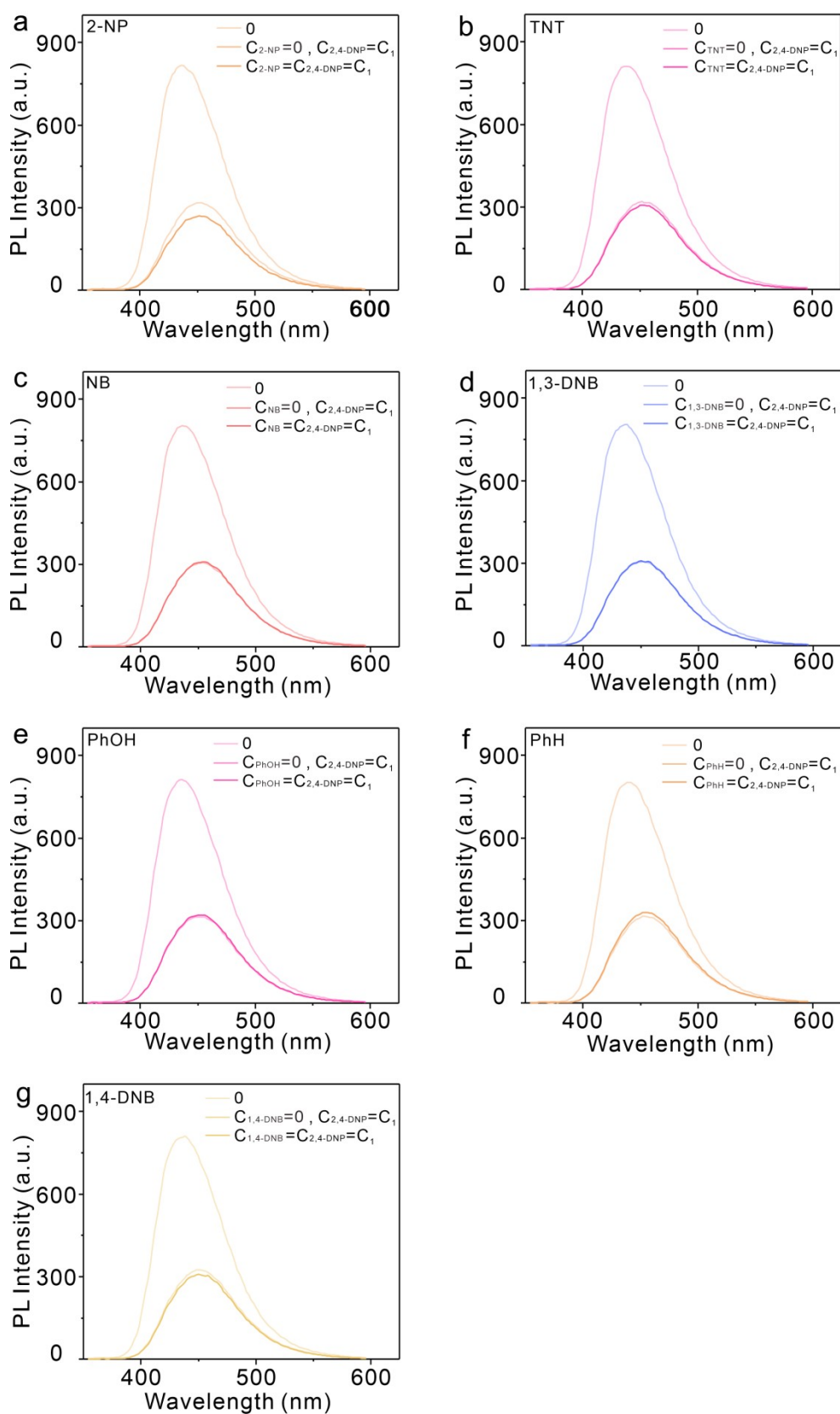
99

100 **Fig. S7.**  $(I_0 - I)/I_0$  values (i.e., quenching efficiency) of  $\text{NH}_2\text{-MIL-125(Ti)}$  suspension in  
101 the presence of different aromatic compounds (310  $\mu\text{M}$ ).

102

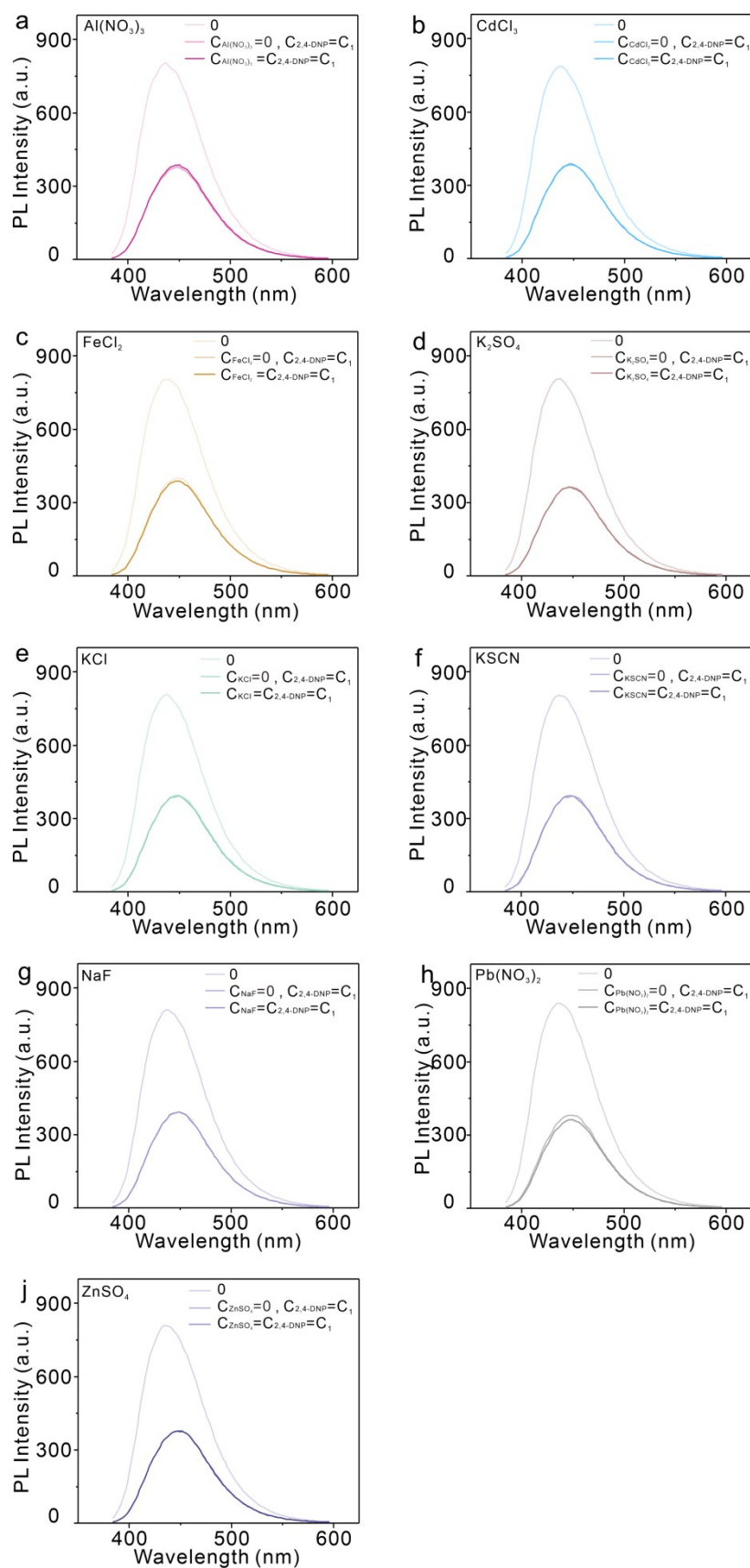
103





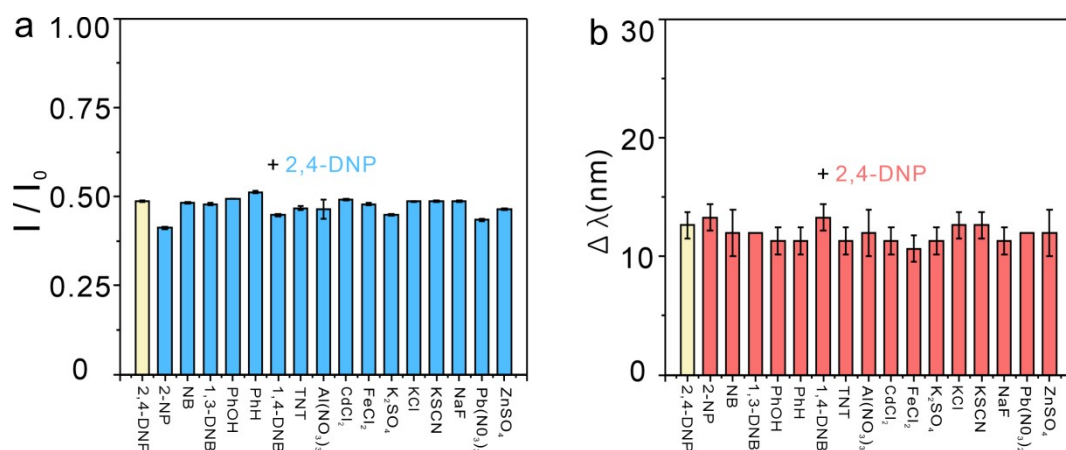
104

105 **Fig. S8.** PL emission spectra of  $\text{NH}_2\text{-MIL-125(Ti)}$  in the presence of 2,4-DNP and (a)  
 106 2-NP, (b) TNT, (c) NB, (d) 1,3-DNB, (e) PhOH, (f) PhH and (g) 1,4-DNB upon  
 107 excitation at 334 nm.



108

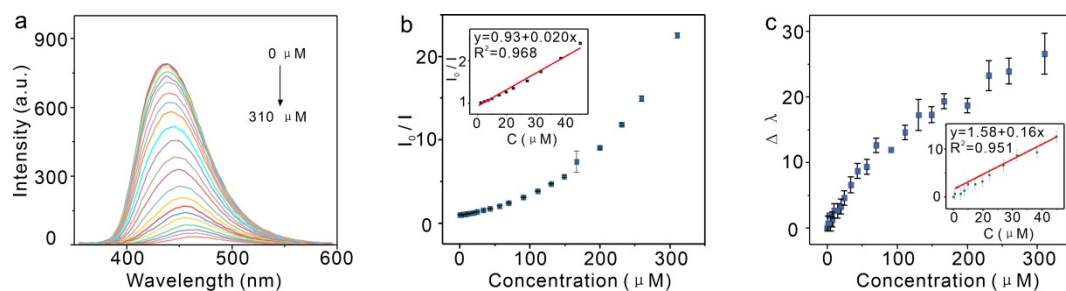
109 **Fig. S9.** PL emission spectra of  $\text{NH}_2\text{-MIL-125(Ti)}$  in the presence of 2,4-DNP and (a)  
 110  $\text{Al(NO}_3)_3$ , (b)  $\text{CdCl}_2$ , (c)  $\text{FeCl}_2$ , (d)  $\text{K}_2\text{SO}_4$ , (e)  $\text{KCl}$ , (f)  $\text{KSCN}$ , (g)  $\text{NaF}$ , (h)  $\text{Pb(NO}_3)_2$   
 111 and (j)  $\text{ZnSO}_4$  upon excitation at 334 nm.



112

113 **Fig. S10.** The anti-interference test of  $NH_2$ -MIL-125(Ti) in the detection of 2,4-DNP:  
 114 (a)  $I_0/I$  and (b)  $\Delta\lambda$ , the yellow color represents the presence of only 2,4-DNP (50  $\mu M$ ),  
 115 while the blue and red colors indicate the coexistence of both 2,4-DNP (50  $\mu M$ ) and  
 116 interfering substances (50  $\mu M$ ).

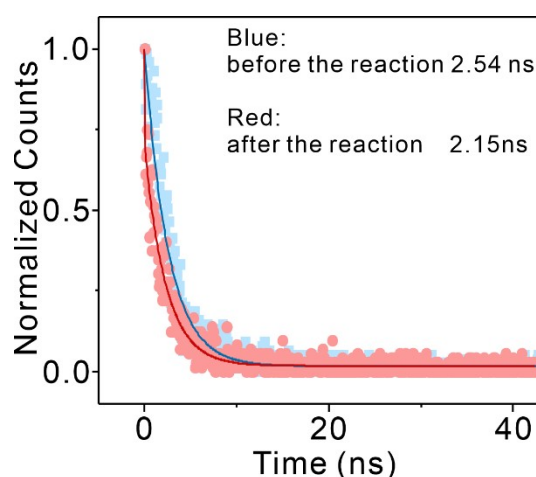
117



118

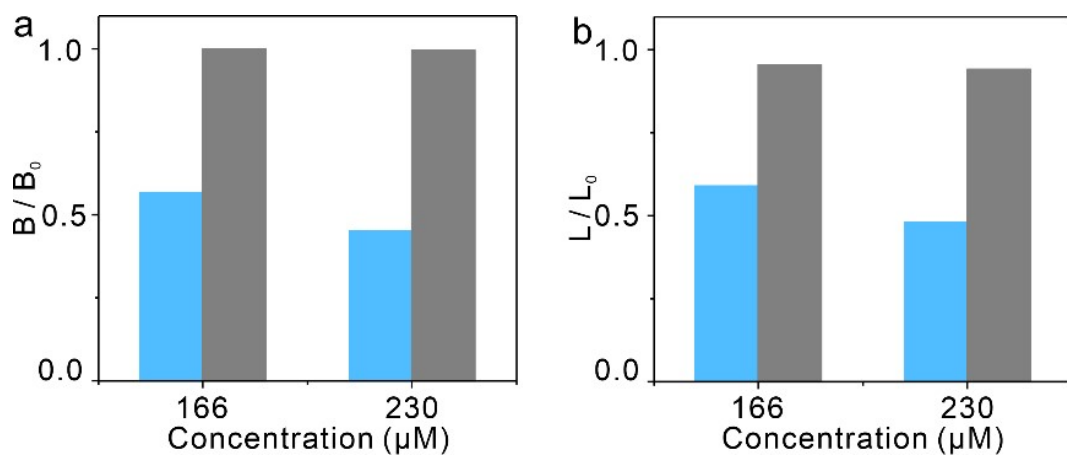
119 **Fig. S11.** A real sample test was conducted in tap water, (a) PL emission spectra of  
 120  $NH_2$ -MIL-125(Ti) were observed in the presence of varying concentrations of 2,4-  
 121 DNP, (b) the relationship between  $I_0/I$  and concentration of 2,4-DNP, (c) the  
 122 relationship between  $\Delta\lambda$  and concentration of 2,4-DNP.

123



124

125 **Fig. S12.** Fluorescence lifetime of  $NH_2$ -MIL-125(Ti) before and after reaction with 70  
 126  $\mu M$  2,4-DNP.



127

128 **Fig. S13.** (a) The relationship between  $B/B_0$ , (b)  $L/L_0$  values and different  
 129 concentrations of 2,4-DNP (blue) and 1,4-DNB (gray) (B and L values were identified  
 130 by APP *Color Detector* under the irradiation of 365nm UV lamp).

131

132 **References**

- 133 1 L. Chen, Z. Cheng, X. Peng, G. Qiu and L. Wang, *Anal. Methods-UK*, 2022, **14**,  
134 44-51.
- 135 2 X. S. Wang, L. Li, D. Q. Yuan, Y. B. Huang and R. Cao, *J. Hazard. Mater.*,  
136 2018, **344**, 283-290.
- 137 3 Q. Hu, T. Xu, J. Gu, L. Zhang and Y. Liu, *CrystEngComm*, 2022, **24**, 2759-2766.
- 138 4 J. Yan, A. D. Carl, A. R. Maag, J. C. MacDonald, P. Müller, R. L. Grimm and S.  
139 C. Burdette, *Dalton. Trans.*, 2019, **48**, 4520-4529.
- 140 5 J. Wang, Q. Zha, G. Qin and Y. Ni, *Talanta*, 2020, **211**.
- 141 6 J. Zhang, Y. Deng, S. Wang, J. Yang and S. Hu, *CrystEngComm*, 2023, **25**,  
142 1495-1500.
- 143